Deep–Sea Research I 199 (2023) 104110

Contents lists available at ScienceDirect

Deep-Sea Research Part I

journal homepage: www.elsevier.com/locate/dsri

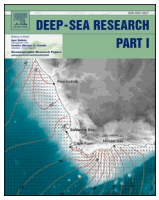

Chloeia rozbaczyloi, a new species of polychaete (Archinominae: Amphinomidae) and first record of the family for the Nazca Ridge, southeastern Pacific Ocean☆

Juan I. Cañete [a], María S. Romero [b], Erin E. Easton [c,d], Ariadna Mecho [d,e], Javier Sellanes [d,f,*]

[a] Departamento de Ciencias y Recursos Naturales, Facultad de Ciencias, Universidad de Magallanes, Punta Arenas, Chile
[b] Laboratorio Microscopia Electrónica, Facultad de Ciencias del Mar, Universidad Católica del Norte, Coquimbo, Chile
[c] School of Environmental, Earth, and Marine Sciences, University of Texas Rio Grande Valley, Brownsville, TX, USA
[d] Center for Ecology and Sustainable Management of Oceanic Islands (ESMOI), Universidad Católica del Norte, Coquimbo, Chile
[e] Barcelona Supercomputing Center, Barcelona, Spain
[f] Departamento de Biología Marina, Facultad de Ciencias del Mar, Universidad Católica del Norte, Coquimbo, Chile

ARTICLE INFO

Keywords:
Fireworm
Deep sea
Seamount
Nazca-desventuradas marine park
Chile
Archinomidae

ABSTRACT

The amphinomid polychaete *Chloeia rozbaczyloi* sp. nov., collected from seamounts of the Nazca Ridge (NR), northwest of Desventuradas islands, southeastern Pacific Ocean, is described. The new species was observed on only two of seven seamounts surveyed in the area (25.079°S, 82.006°W, and 25.408°S, 81.769°W, ~220 m depth), being abundant on one of them.

Specimens were observed under optical and scanning electron microscopes, and DNA was sequenced (COI, 16S, 18S, and 28S nucleotide alignment). *Chloeia rozbaczyloi* sp. nov. belongs to the *venusta* group of *Chloeia* and is distinguished mainly by: (i) the chromatic pattern of the dorsum (with a single middorsal dark band) and the caruncle (with 16–20 vertical folds and 12 to 14 black spots posteriorly decreasing in diameter), (ii) by the bi-annulated dorsum of the first ten chaetigers, each with a bean-shaped anterior pseudosegment, (iii) long neuropodial cirri, with a short ceratophore, at chaetiger 2 and reaching chaetiger 6, and (iv) bipinnate branchiae from chaetiger 4, with seven to nine lateral branches arising from the primary axis, each possing five pinnules; branchiae change progressively in size to the posterior end. The ciliated margin of the accessory dorsal cirri suggests a respiratory function that might be relevant considering that both seamounts in which the species was observed could be influenced by low-oxygen waters. DNA results further support that *C. rozbaczyloi* sp. nov. differs from the other five congeneric taxa (*C. bimaculata*, *C. flava*, *C. parva*, *C. pocicola*, and *C. viridis*) for which genetic information is available.

This finding constitutes the first report of the genus for Chilean waters, increasing the number of species of Amphinomidae in this area to seven. It also confirms the presence of the family in the NR and increases the number of *Chloeia* species in the world to 43.

The seamounts where the new species have been collected are within the newly created offshore Nazca-Desventuradas Marine Park. Information on potentially unique and endemic species, such as the one discussed here, is of utmost importance to preserve special ecological units, address ecosystem services, and implement management measures in the area.

1. Introduction

Chloeia Lamarck, 1818 is one of the 18 recognized genera of Amphinomidae (Polychaeta), known as fireworms for the burning sensation felt by humans in response to exposure to the setal-associated neurotoxin produced by some species (Kudenov, 1995). Although the family is distributed globally in most marine environments (Kudenov, 1995; Rouse and Pleijel, 2001; Böggemann, 2009; Wang et al., 2019; Yáñez-Rivera and Salazar-Vallejo, 2022; Salazar-Vallejo, 2023), *Chloeia* species have a more circumtropical distribution, occurring mostly at shallow depths and being more speciose in the Indian and Pacific than in

☆ This article is registered in ZooBank under urn:lsid: zoobank.org:pub:3F142A93-1679-4192-AA75-8B71CA0A79F4.

* Corresponding author. Center for Ecology and Sustainable Management of Oceanic Islands (ESMOI), Universidad Católica del Norte, Coquimbo, Chile.
E-mail address: sellanes@ucn.cl (J. Sellanes).

https://doi.org/10.1016/j.dsr.2023.104110
Received 5 September 2022; Received in revised form 10 July 2023; Accepted 13 July 2023
Available online 15 July 2023

Abbreviations

CIMAR	Program for Oceanographic Exploration of Remote Jurisdictional Marine Areas, funded by the National Oceanographic Committee of Chile, Chilean Navy
BL	Body length
MNHNCL	Museo Nacional de Historia Natural, Santiago, Chile.
NDMP	Nazca-Desventuradas Marine Park
NR	Nazca Ridge
OMZ	Oxygen Minimum Zone
ROV	Remotely Operated Vehicle
SCBUCN	Sala de Colecciones Biológicas, Universidad Católica del Norte, Facultad de Ciencias del Mar, Coquimbo, Chile.
SEM	Scanning Electron Microscope

the Atlantic Ocean (Salazar-Vallejo, 2023). *Chloeia* species are characterized by having an elliptical body, with bipinnate branchiae (Barroso and Paiva, 2011), notopodial cirri, cirrophores, and a caruncle (Kudenov, 1995; Barroso et al., 2021). They have species-specific dorsal pigmentation patterns, which are often violet, green, yellow, black, and reddish brown/black (Kudenov, 1995; Yáñez-Rivera and Salazar-Vallejo, 2022). Other taxonomically informative characters include relative size and development of the caruncle; length of second parapodial cirri; chaetae number, distribution along body, and shape; types of notochaetae, neurochaetae, and pygidial cirri; distribution, development, and placement of branchiae; degree of development and type of anal cirri as a proportion of sizes of the eyes; and caruncle pigmentation pattern (Kudenov, 1995; Barroso and Paiva, 2011; Wang et al., 2019; Yáñez-Rivera and Salazar-Vallejo, 2022; Salazar-Vallejo, 2023). Polychaetes are known to have significant changes in the size of eyes, shape of parapodia, caruncle pigmentation and chaetae during epitoky period (Rouse and Pleijel, 2001), especially in amphinomids (Salazar-Vallejo, 2023). Most *Chloeia* species have branchiae beginning from the chaetiger 4 (Table 1); species with branchiae beginning from chaetiger 5 have been reported for the southern parts of the Indian and Pacific oceans (Barroso and Paiva, 2011; Barroso et al., 2021; Yáñez-Rivera and Salazar-Vallejo, 2022; Salazar-Vallejo, 2023).

Except for a single mention of the genus *Chloeia* for some seamounts of the Salas y Gómez Ridge by Parin et al. (1997), no species of the genus have been reported for other seamounts or ocean ridges worldwide, despite some *Chloeia* occurring in the deep-sea (Barroso and Paiva, 2011). The latter include the recently described *C. pocicola* from pockmark fields off the Brazilian coast at ~750 m depth (Barroso et al., 2021) and *C. pinnata*, which shows a wide bathymetric distribution ranging from 20 to 1900 m depth (Jones and Thompson, 1987; Yáñez-Rivera and Salazar-Vallejo, 2022). Of the 42 currently accepted species (Wang et al., 2019; Read and Fauchald, 2022; Barroso et al., 2021; Yáñez-Rivera and Salazar-Vallejo, 2022; Salazar-Vallejo, 2023), nine occur in the Atlantic Ocean (including the Mediterranean Sea), 12 in the Indian Ocean, 13 in the Indo-west Pacific, and seven in the eastern or southern Pacific Ocean. Of the species at least partially distributed in the Pacific Ocean, five have been described from the northwestern Pacific (*C. bimaculata*, *C. conspicua*, *C. fusca*, *C. incerta,* and *C. pulchella*), seven from the central and the eastern Pacific (*C. fusca*, *C. murrayae*, *C. nuriae, C. pinnata, C. poupini, C. pseuglochis* and *C. richeri*), and one from the southern Pacific (*C. inermis*) (Yáñez-Rivera and Salazar-Vallejo, 2022; Salazar-Vallejo, 2023). Before the present study, only six species of Amphinomidae were reported from Chilean waters (Kudenov, 1993; Rozbaczylo 1985; Cañete 2017); half of them for Rapa Nui (Easter Island) [i.e., *Eurythoe complanata* (Pallas, 1776), *Pherecardia striata* (Kingberg, 1857) and *Linopherus* sp. (Kohn and Lloyd, 1973; Cañete, 2017)]. The other three species, *Paramphinome australis* Monro, 1930, *Pareurythoe chilensis* (Kingberg, 1857), and *Linopherus annulata* Hartmann-Schröder, 1965, are respectively distributed between Arica (northern Chile) and Antarctica (25–1180 m depth), between Valparaíso and Chiloé Island (13–260 m depth), and around Mocha Island and Galera Point (26–160 m depth) (Rozbaczylo, 1985). No prior reports of the family exist in the literature for the Nazca Ridge (NR) seamounts and islands, a zone that seems to be prolific in new species of polychaetes (Díaz-Díaz OF et al., 2020).

In this study, we (i) describe *Chloeia rozbaczyloi* sp. nov, the first species of the genus reported for seamounts of the NR within Chilean jurisdiction, (ii) provide preliminary information on its abundance and habitat, and (iii) provide some insight into the function of the accessory dorsal cirri. In addition, we provide sequence data for the partial mitochondrial genome and 18S-to-28S rRNA gene fragment and infer the genetic relationship between *C. rozbaczyloi* sp. nov. and other congeneric species based on available genetic data.

2. Materials and methods

During the multidisciplinary oceanographic cruise CIMAR 22 "Oceanic Islands", carried out onboard RV *Cabo de Hornos* between October and November 2016, the benthic habitat and fauna of unexplored seamounts of the Juan Fernández and Desventuradas Ecoregion (Spalding et al., 2007; ecoregion number 179) were surveyed by remotely operated vehicle (ROV) and from bottom trawling (Tapia-Guerra et al., 2021, Tapia-Guerra et al., 2021) (Fig. 1). Habitat characterizations and relative abundance of the benthic epifauna were performed from video observations using an ROV (model Commander MKII, Mariscope Meerestechnik, Kiel, Germany) equipped with an HD Camcorder (Panasonic SD 909) and laser pointers (10 cm apart). A total of 11 video transects were performed within the NDMP between 130 and 370 m depth; six transects at NR seamounts and five around the Desventuradas Islands (Fig. 1A). After ROV surveys, samples were collected by 10-min hauls (bottom contact), at ~3 knots, using a modified Agassiz trawl that consisted of a metal frame with a mouth of 2 × 0.5 m (width × height) fitted with a net of 12-mm mesh at the cod end.

Individuals of a locally abundant fireworm belonging to the Amphinomidae were observed and collected at seamount SFX (Fig.1 B), one of the seven seamounts surveyed during the cruise (Fig. 1). Collected specimens were preserved in 100% ethanol. Additional specimens were subsequently collected, following the same collection and preservation methods, from ~250 m depth at another seamount (SPG4; Fig. 1) located ~22 nm southeast of the original locality (seamount SFX). This seamount was the only seamount of the NR surveyed during the EPIC (Eastern Pacific International Campaign) cruise (RV *Mirai*). Sample collection was done under the permission Res. Ext N°3685/2016 and N°4508/18 from SUBPESCA (Chile) to Universidad Católica del Norte. All specimens were preserved onboard following the protocols described above and initially deposited at SCBUCN.

The following morphological characters were examined: maximum body width (excluding chaetae), body length (prostomium to pygidium), number of chaetigers, length, shape, number of vertical folds, and free posterior zone of the caruncle, size along the body and number of lateral branches and pinnules in each lateral branch, number of accessory dorsal cirrus, size of ventral cirri, chaetal lobes, chaetal shapes and changes along the body, and dorsal chromatic pattern. Cephalic terminology follows Orrhage (1990), Kudenov (1993, 1995), Barroso and Paiva (2011), Borda et al. (2015), and a recent proposal by Yáñez-Rivera and Salazar-Vallejo (2022) and Salazar-Vallejo (2023). The taxonomic description of amphinomid specimens was based on Kudenov (1993), Liñero-Arana and Díaz (2010), Borda et al. (2012, 2015), Wang et al. (2019), Barroso et al. (2021), Yáñez-Rivera and Salazar-Vallejo (2022), and Salazar-Vallejo (2023). The general description was performed under stereoscopic microscopy and is based on a 35-mm-long specimen (Holotype MNHNCL ANN-15017). Additional specimens (paratypes SCBUCN 6981–6984) were examined and photographed under a Hitachi

Table 1
Main taxonomic features of *Chloeia* Savigny in Lamarck, 1818 (Polychaeta: Amphinomidae: Archinominae): type of branchiae (pinnate vs. bipinnate), chaetiger number (3, 4 or 5) in which branchiae start, and the dorsal pigmentation pattern (single middorsal bands, single middorsal spots, double longitudinal bands, complex patterns, or none). Numbers indicated in parenthesis for each *Chloeia* group, according to Salazar-Vallejo (2023), correspond to the number of species in each group. Modified from Salazar-Vallejo, (2023). The species described here is bolded. References: Yáñez-Rivera and Salazar-Vallejo (2022), Salazar-Vallejo (2023), and present study.

Main branchiae taxonomic feature	Chaetiger number in which branchiae start	Branchiae size characteristics	*Chloeia* group	Dorsal band characteristics	*Chloeia* species
Branchiae pinnate			*rosea* (1)		*C. rosea* Potts 1909
Branchiae bipinnate	3		*fucata* (1)		*C. fucata* de Quatrefages 1866
	4	Branchiae progressively smaller posteriorly	*flava* (3)	Middorsal spots	*C. flava* (Pallas 1766)
					C. maculata Potts 1909
					C. pulchella Baird 1868
			venusta (5)	Middorsal band	*C. nuriae* Yáñez-Rivera and Salazar-Vallejo (2022)
					C. piotrowskiae Salazar-Vallejo, 2023
					C. poupini Salazar-Vallejo (2023)
					***C. rozbaczyloi* Cañete & Sellanes 2023**
					C. venusta de Quatrefages 1866
			viridis (12)	Dorsum with complex patterns of pigmentation	*C. amoureuxi* Salazar-Vallejo (2023)
					C. amphora Horst, 1912
					C. conspicua Horst, 1912
					C. euglochis Ehlers 1887
					C. gilleti Salazar-Vallejo (2023)
					C. *hutchingsae* Salazar-Vallejo (2023)
					C. incerta de Quatrefages 1866
					C. meziane Salazar-Vallejo (2023)
					C. pseudeuglochis Augener 1922
					C. violacea Horst, 1912
					C. viridis Schmarda 1861
					C. zibrowii Salazar-Vallejo (2023)
			tumida (13)	Dorsum without pigmentation pattern	*C. bemisae* Salazar-Vallejo (2023)
					C. boucheti Salazar-Vallejo (2023)
					C. entypa Chamberlin 1919
					C. fauveli Salazar-Vallejo (2023)
					C. fiegei Salazar-Vallejo (2023)
					C. gesae Salazar-Vallejo (2023)
					C.gilchristi McIntosh 1924
					C. keablei Salazar-Vallejo (2023)
					C. murrayae Salazar-Vallejo (2023)
					C. paulayai Yáñez-Rivera and Salazar-Vallejo (2022)
					C. pinnata Moore 1911
					C. richeri Salazar-Vallejo, (2023)
					C. tumida Baird, 1868
		Branchiae abruptly smaller after a few chaetigers	*kudenovi* (2)		*C. kudenovi* Barroso and Paiva (2011)
					C. pocicola Barroso & Kudenov (Barroso et al., 2021)
	5		*fusca* (2)	Double middorsal bands	*C. bistriata* Grube 1868
					C. fusca (McIntosh 1885)
			longisetosa (4)	Dorsum without pigmentation pattern	*C. inermis* de Quatrefages 1866
					C. longisetosa Potts 1909
					C. slapcinskyi Salazar-Vallejo (2023)
					C. wangi Salazar-Vallejo (2023)

SU3500 scanning electron microscope (SEM) at the Microscopy Laboratory of the Facultad de Ciencias del Mar, Universidad Católica del Norte, Coquimbo, Chile. Specimens examined with SEM were fixed in ethanol, dehydrated through a graded ethanol series, dried in a Tousimis, Samdri-780A critical-point dryer using CO_2, mounted on bronze stubs, and coated with gold in a JEOL JFC-100 evaporator. The type material was deposited in the MNHNCL and SCBUCN, including specimens prepared for SEM analysis. The description is complemented by observations of living specimens in their natural habitat as documented by images taken by ROV (Fig. 2).

DNA was extracted from specimen SCBUCN 6857 using a PureLink Genomic DNA Purification Kit (Invitrogen, Waltham, Massachusetts, USA) per manufacturer's protocol, with a 60-min incubation (55 °C at 700 rpm) in a Thermomixer (Eppendorf, Hamburg, Germany) and elution with 50 μl of nuclease-free water. Extracted DNA was submitted to Biopolymers Facility at Harvard Medical School for library preparation (Illumina Nextera XT2) and next-generation sequencing (NextSeq 500). The *18S-ITS1-5.8S-ITS2-28S* fragment was recovered following Easton and Hicks (2020) by using software installed on the University of New Hampshire Bioinformatics Core facility RON server, which is supported by the New Hampshire-INBRE Program through an Institutional Development Award, P20GM103506, from the National Institute of General Medical Sciences of the NIH and Geneious Prime 22.0.1 (https://www.geneious.com). Because the complete mitochondrial genome was not recovered by those methods, reads were iteratively mapped to *C. pocicola* (MT822294) mitochondrion (complete genome), which is the

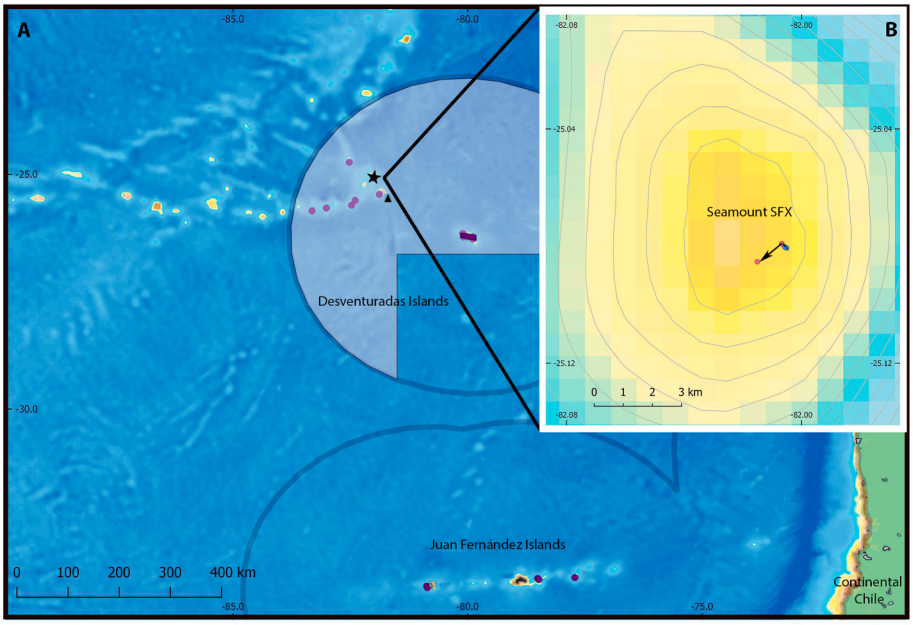

Fig. 1. Study area and sampling points at the Nazca Ridge and Juan Fernández archipelago during CIMAR 22 and EPIC cruises. **A** Star indicates the location of seamount SFX, the seamount in which the species *Chloeia rozbaczyloi* sp. nov. has been reported of all the seamounts sampled during CIMAR 22 (violet dots), and the triangle indicates SPG4, the seamount in which additional material of the new species was collected during the EPIC cruise. **B** Blue dot indicates the initial position of the ROV transect and red dots the initial and final position of the trawl transect at seamount SFX.

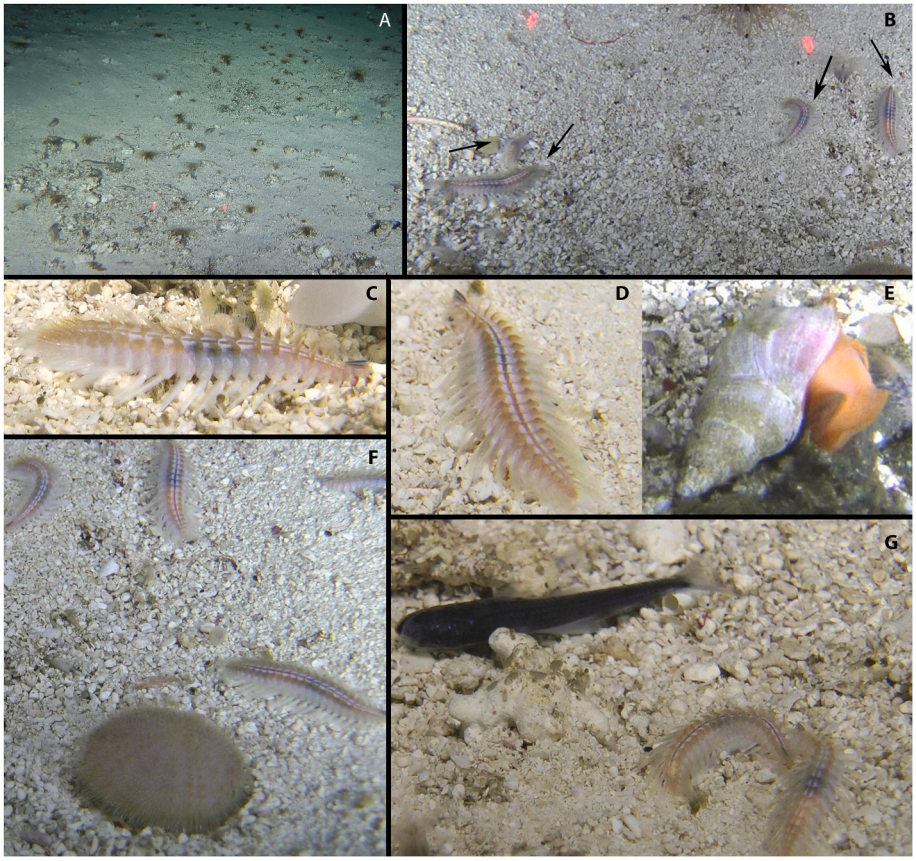

Fig. 2. Frames extracted from the ROV videos obtained at the seamount SFX with *in situ* observations of *Chloeia rozbaczyloi* sp. nov. **A** Representative image of the habitat, dominated by calcareous coarse sediment and rhodoliths, dark spots are small anemones; **B** *Chloeia rozbaczyloi* sp. nov. on the substrate near an anemone; **C, D** close-ups of *Chloeia rozbaczyloi* sp. nov. showing live coloration; **E** an individual next to the gastropod *Chryseofusus kazdailisi;* **F** individuals near the irregular echinoid *Scrippsechinus fisheri*; **G** a dead fish, probably a myctophid, close to two *Chloeia rozbaczyloi* sp. nov. individuals. Distance between the red dots of the laser pointers in **A** and **B** is 10 cm.

only complete mitochondrial genome for *Chloeia*, and the resulting consensus sequences with Geneious Prime. Details of these methods and more expansive genetic methods are available in the Supplementary Material. The partial mitochondrial genome and the *18S-ITS1-5.8-S-ITS2-28S* fragment were annotated with Live Annotate and Predict in Geneious, respectively, with annotations from *C. pocicola* and *Panthalis oerstedi* (KY753846). Results from the MITOS Webserver (http://mitos.bioinf.uni-leipzig.de/index.py; Bernt et al., 2013) were used to modify the position of the tRNAs. Protein and rRNA gene annotations were manually adjusted based on alignment with *C. pocicola* genes and congruency in presence of predicted start and stop codons between the species. The annotated mitogenome and unannotated *18S-ITS1-5.8-S-ITS2-28S* were submitted to GenBank (OM144973 and OM135245, respectively). For the mitochondrial genome sequence, percentage

identity between *C. pocicola* and *C. rozbaczyloi* sp. nov. nucleotide and amino acid sequences were calculated based on MUSCLE nucleotide and Geneious amino acid alignments as implemented in Geneious Prime with default parameters; stop codons and missing bases and amino acids were excluded from the alignments, which were trimmed to the shortest extent of aligned genes.

For phylogenetic reconstruction based on a concatenated alignment of *28S* rRNA, *16S* rRNA, and *COI* gene fragments, we selected one representative from each *Chloeia, Archinome,* and *Notopygos* species for which sequences were available for each of the three gene regions; *Paramphinome jeffreysii* was selected as the outgroup for all reconstructions (Supplementary Material Table S1). Although *18S* rRNA gene fragments were publicly available for most representatives, this gene was excluded from the study because some sequences were missing data or were suspect based on large divergences from the other representatives and most remaining representatives had identical haplotypes for congeners, so the *18S* rRNA gene fragment lacked informative characters for species-level assignments. Sequences were aligned with default Muscle parameters as implemented by Geneious Prime and trimmed to their shortest extent. Genetic similarities (uncorrected p) are reported based on the concatenated and single-gene alignments. Following Xia et al. (2003) and Xia and Lemey (2009), the third codon position of the *COI* gene was removed before phylogenetic reconstruction, leaving a 394 bp alignment, because this codon position was saturated ($p = 0.0096$, $I_{ss} = 0.7278$, $I_{ss.c} = 0.6409$) as determined by the Xia et al. (2003) test of substitution saturation in DAMBE7 (Xia 2018) and therefore is not useful in phylogenetic reconstruction. These single-gene alignments were concatenated (28S + 16S + COI) in Geneious Prime into a 1452 bp alignment (735 + 323 + 394 bp, respectively), and the best model of nucleotide evolution was selected with PartitionFinder 2.1.1 (Lanfear et al., 2017) with the following settings: branchlengths = unlinked, models = all with –raxml code (Stamatakis, 2014), model_selection = aicc, search = greedy (Lanfear et al., 2012), and data blocks defined to each gene boundary with protein-coding genes split into the two codon positions for a total of four data blocks. The best scheme selected was to retain the four data blocks as separate partitions with GTR + G selected as the model for *COI* codon position 2 and GTR + I + G as the model for the other three partitions. Because RAxML allows only a single model of rate heterogeneity in partitioned analyses and GTRG + I + G was selected for most partitions, the maximum-likelihood (ML; Felsenstein, 1981) phylogenetic tree was constructed in RAxML 8.2.11 (Stamatakis 2014) with nucleotide model = GTR GAMMA I, 100 bootstrap replicates (rapid bootstrapping with a search for best-scoring ML tree), and no outgroup. The best models and partitions were used as prior parameters to reconstruct phylogenies with MrBayes 3.2.6 (Huelsenbeck and Ronquist, 2001) as implemented by Geneious Prime with the selected outgroup (*Paramphinome jeffreysi*), 10,000,000 generations, sample frequency of 1000, 4 Markov Chain Monte Carlo, a temperature of 0.2, and burnin of 2500. The final trees were obtained with a 50% majority-rule consensus, and bootstrap values from RAxML phylogenetic trees were added to the nodes. Commands for all phylogenetic reconstructions and details of single-gene phylogenetic reconstructions are available in the Supplementary Material.

This published work and the nomenclatural acts it contains were registered in ZooBank (LSID urn:lsid:zoobank.org:pub:3F142A93-1679-4192-AA75-8B71CA0A79F4).

3. Results

Collections and habitat. At seamount SFX (Figs. 1), 64 specimens were collected on 31 Oct 2016 at ~230 m depth. *Chloeia rozbaczyloi* sp. nov. was abundant (Fig. 2A–G), usually patched in small groups with maximums of ~7 specimens per 100 cm^2. Sea-bottom observations at seamount SFX revealed calcareous sediments produced by foraminiferous tests, debris of deep-sea corals, holopelagic gastropod shells, and rhodoliths (Fig. 2A–D). Other taxa representative of this station were anthozoans (unidentified anemones, Fig. 2A–B), a fasciolarid gastropod (*Chryseofusus kazdailisi*, Fig. 2E), and the irregular echinoid *Scrippsechinus fisheri* (Fig. 2F).

3.1. Systematics

Family Amphinomidae Lamarck, 1818.

Subfamily Archinominae Kudenov, 1991.

Genus ***Chloeia*** Lamarck, 1818.

Type species. *Aphrodita flava* Pallas, 1766, accepted as *Chloeia flava* (Pallas, 1766) by subsequent designation.

***Chloeia rozbaczyloi* sp. nov.** Cañete and Sellanes.

Fig. 2 B-D, F, G; 3 A-F; 4 A-G; 5; 6 A-G; 7; 8; Table 1; Supplementary Material.

LSID urn: lsid: zoobank.org:act:574C45FA-EBE7-4614-AB33-E5B9E21CA3F3.

Material examined. Eight specimens: Holotype (MNHNCL ANN-15017) and seven paratypes (SCBUCN 6981–6984, 6857, 6859, and 7262) from seamount SFX, 25.079°S, 82.006°W, Agassiz trawl, 220–230 m depth, *RV Cabo de Hornos*, CIMAR 22 cruise, 31 Oct. 2016. Additional material: 22 specimens (SCBUCN 8529), all from unnamed seamount Sta. SPG4, 25.408°S, 81.769°W, Agassiz trawl, ~211 m depth, RV *Mirai*, EPIC cruise, 2 Feb. 2019.

Diagnosis. Body fusiform, with 30 segments. Anterior ten chaetigers with central dorsum bi-annulated; complete segment dorsally separated by an anterior bean-shaped pseudosegment; dark middorsal band surrounded by white areas. Trilobate caruncle extending to chaetiger 4, fused to dorsum on chaetigers 1 to 2, free thereafter; with median plicate lobe with 16–20 vertical folds and 10 to 14 black spots decreasing in size toward the posterior end; first two black spots hourglass shaped. First three chaetigers with an accessory dorsal cirrus; accessory dorsal cirrus without ceratophores and lateral margin of mid-central region ciliated. Bipinnate branchiae from chaetiger 4, progressively smaller towards posterior region; bifucarte harpoon notochaetae without spurs; thin furcate neurochaetae. Neuropodial cirri of second chaetiger long, with short ceratophore, reaching chaetiger 6.

Type locality. Seamount SFX, at ~230 m depth. Initial geographic position: 25.079°S, 82.006°W; final position 25.085°S, 82.015°W. 31 Oct. 2016.

Description. Holotype (MNHNCL ANN-15017), complete specimen BL of 35 mm by 9 mm wide (excluding chaetae) in the middle of the body, 28 chaetigers. Specimen with body dorsally flattened, depressed, oval, whitish alive, with gills brown to violet in color; caruncle black, with white band in the lateral margin; all cirri, antennae, and palps whitish. Notochaetae transparent while neurochaetae are whitish; neurochaetae longer than notochaetae. Mid-body dorsum slightly darker than anterior and posterior segments (Fig. 2B, C, F, G). Specimens preserved in alcohol white, with the mid-funnel ventral zone slightly dark (3A-B). Paratypes SCBUCN 6981, 6982, 6983, and 6984 incomplete, sectioned for SEM analysis. Paratype SCBUCN 6859 and 7262 used for stereoscopic microscopy of the anterior end.

Trilobate caruncle extending to chaetiger 4, tapered, slightly twisted (Figs. 3C, 4A and 5A), with median plicate lobe with 16–20 vertical folds and with 10–14 black spots decreasing in size to posterior end; first two black spots slightly hourglass shaped; caruncle fused to dorsum between chaetigers 1 to 2; free thereafter (Figs. 3C, 4A and 5A). Posterior lobe of the prostomium with two pairs of black eyes hidden under the anterior margin of the base of the caruncle; anterior pair larger than posterior pair (2:1 in size proportion) and externally detectable in most preserved specimens (Fig. 5A).

First ten segments dorsally bi-annulated, of which the anterior pseudosegment is smaller (~1:3 in proportion of total segment lenght) and bean-shaped (Fig. 3D). From chaetiger 11 on, dorsal zone of each segment white, divided by a mid, narrow and elongated, screw-shaped dark mark. This feature is evident in live specimens (Fig. 3F).

Median antennae arising from anterior margin of caruncle; palpal

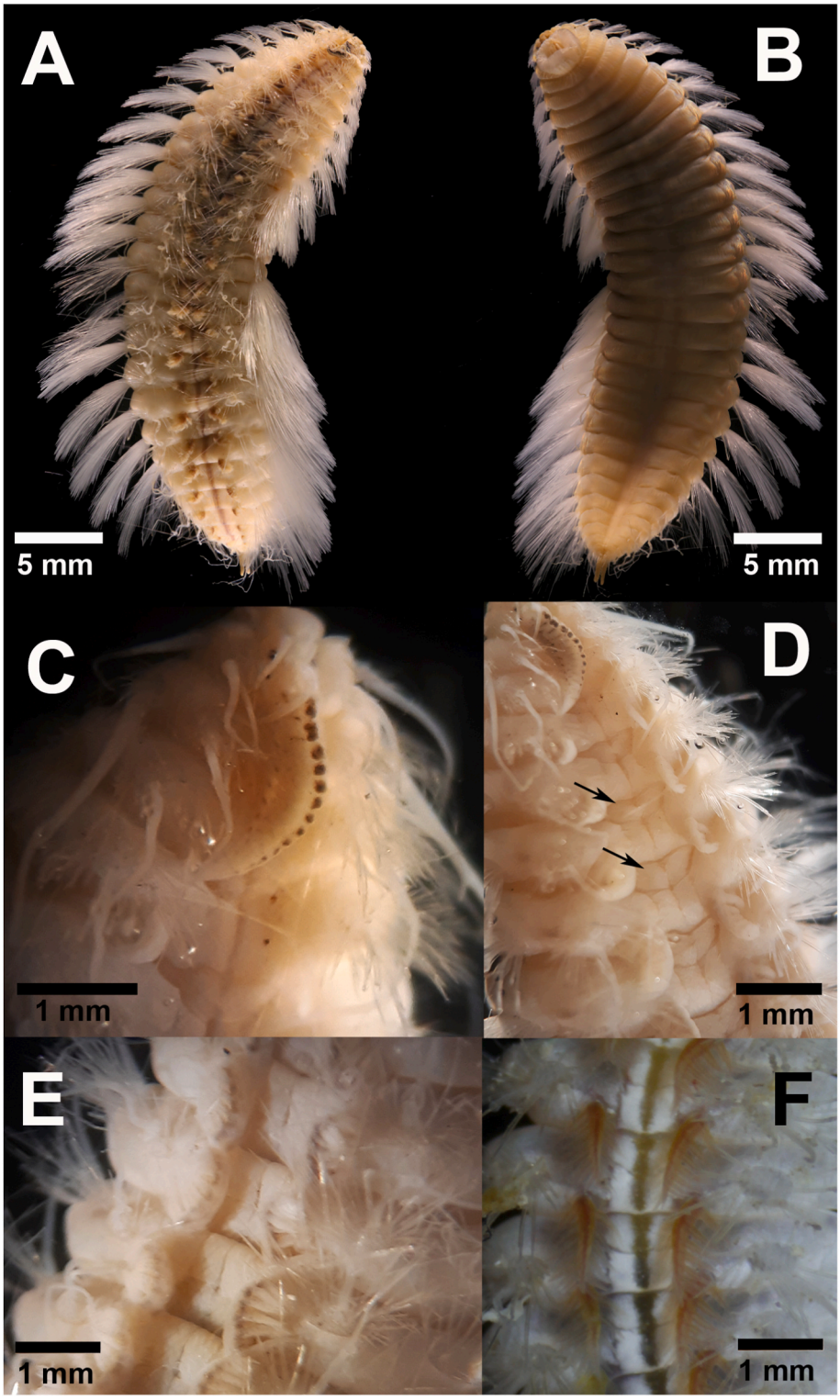

Fig. 3. *Chloeia rozbaczyloi* sp. nov. **A, B** Holotype MNHNCL-ANN-15017, **C, E, F** Paratype SCBUCN-6859, **D** Paratype SCBUCN-7262. **A** whole body dorsal view, and **B** ventral view; **C** dorsal view showing details of the anterior end and the black-spotted pattern of the caruncle; **D** dorsal view of the anterior end showing the difference in the size of the eyes and black-spotted pattern of the caruncle. Note the darker caruncle in this specimen (e = eyes of left side; ca = caruncle; asterisk = anterior lobe of palp). Antennae were removed to show the eyes; **E** dorsal view of chaetigers VIII and IX showing the bean-shaped anterior pseudosegment (black arrows); **F** dorsum of mid chaetigers showing middorsal band, screw-shaped, in a living specimen.

antennae arising from anterior margin of prostomium; lateral antennae anteriorly to median antennae; palpal and lateral antennae of similar length and shape; median antennae longer than paired/palpal antennae (Fig. 4A and B). Median antennae extending to the sixth or seventh folded side of the caruncle or to chaetiger 2; style moderated in length, cylindrical, being shorter than caruncle and of similar length and thickness to lateral antennae; all antennae without ceratophores (Fig. 4B). Palps fused, dorsally ending in a heart shape lobe, semi-grooved; palps converging mid-ventrally into longitudinal groove, leading to mouth (Fig. 4B). Mouth located between palps and posterior lip formed by incomplete segment of second and third chaetigers; posterior margin of buccal area with 5–6 folds anteroposteriorly oriented and projected toward the fourth chaetiger; first two chaetigers of small size, incomplete ventrally and bordering mouth area (Fig. 4C). Ventral cirrus of chaetiger 2 cirriform, longer and wider than the ventral cirrus of the first five chaetigers (4:1 length ratio); ventral cirrus from six to twenty segments long, with styles 5–7 times longer than cirrophore; long ventral cirrus of second chaetiger directed to the dorsal zone and

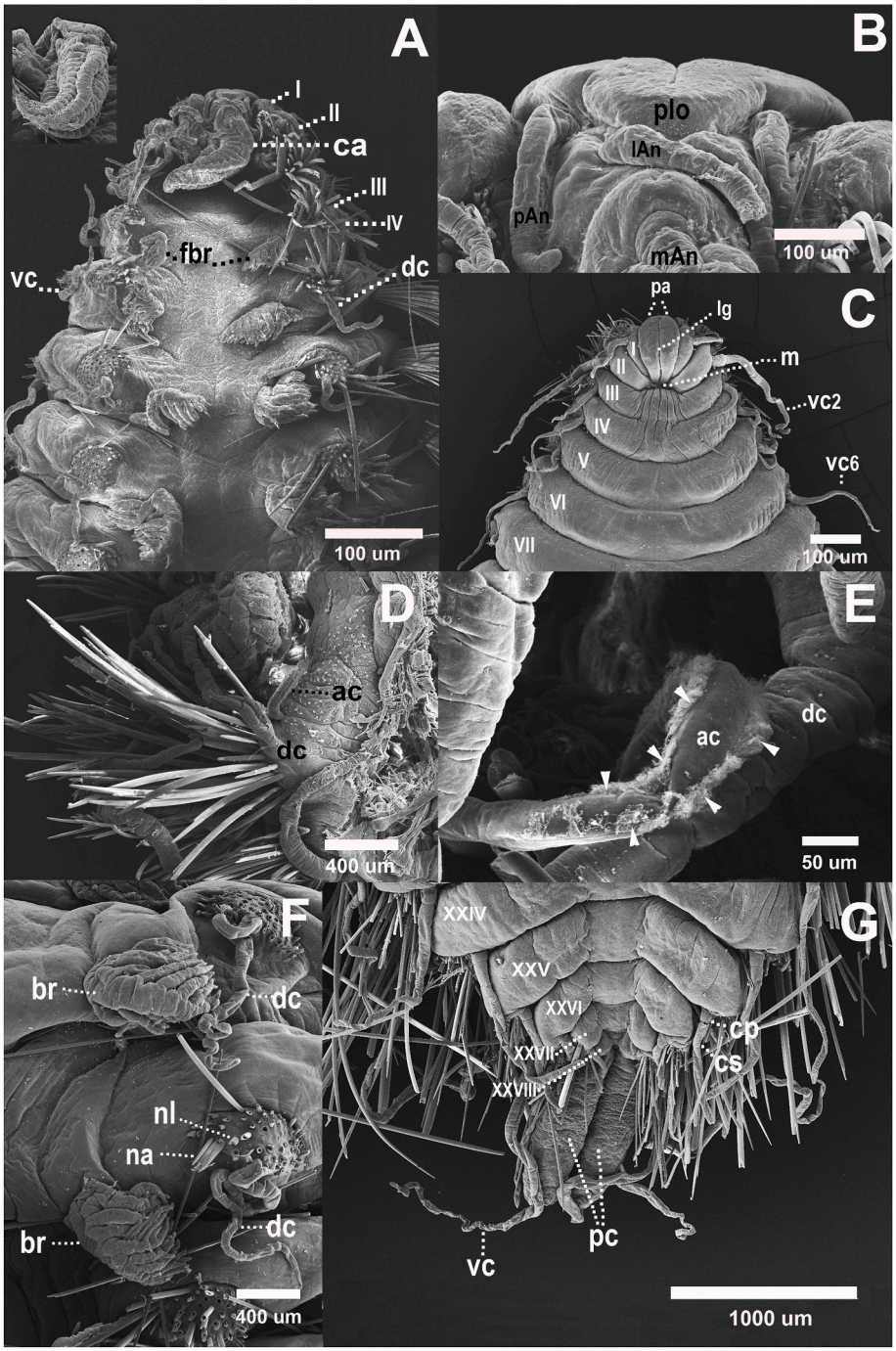

Fig. 4. SEM images of *Chloeia rozbaczyloi* sp. nov. **A** Paratype SCBUCN-6982, **B** paratype SCBUCN-6983, **C, D, F** paratype SCBUCN-6981, **E, G** paratype SCBUCN-6984. **A** dorsal view of the anterior end (ca = caruncle; dc = dorsal cirrus; fbr = first pair of branchiae; vc = ventral cirri; I-IV = chaetigers); detail of caruncle is shown in the left corner, posterior view to shown the free zone and plicated margin; **B** dorsal view of anterior end of prostomium (plo = anterior lobe of palps; IAn = lateral antennae; MAn = Median antennae PAn = Palps antennae; **C** ventral view of anterior end (pa = palps; lg = longitudinal groove; m = mouth; vc2 and vc6 = ventral cirri 2 and 6; I-VII = chaetigers); **D** dorsal view of chaetiger 3 (ac = accessory cirri; dc = dorsal cirri); **E** detail of accessory cirri of chaetiger 3 (white arrows show lateral ciliated margin); **F** dorsal view of branchiate segments (br = branchiae; dc = dorsal cirri; na = notopodial aciculae; nl = notopodial lobe); **G** ventral view of the pygidium showing the aspect of pygidial cirri and its proportion in relation to the last chaetiger and ventral cirrus (pc = pygidial cirri; vc = ventral cirri; cp = ceratophore; cs = ceratostyle; XXIV to XXVIII = five posterior chaetigers).

extending to chaetiger 6 (Fig. 4C).

Dorsal cirri of first three chaetigers with ciliated accessory cirrus that is one-sixth the length of the dorsal cirrus; accessory cirrus without ceratophore; lateral margin of accessory cirrus with ciliated edges; distal end not ciliated (Fig. 4D–E).

Branchiae best developed in mid-chaetigers, decreasing progressively in size to posterior end; branchiae bipinnate from chaetiger 4 to the end of body, in general with seven lateral branches (up to nine in some mid-chaetigers), arising from the primary axis, each having five short pinnules (Figs. 4F and 5B); each branch located in lateral position and well separated from one another; branchiae inserted slightly displaced posterior to the notopodial lobe, close to intersegmental groove (Fig. 4F). Branchiae shorter than dorsal cirrus (1:2) (Fig. 4F).

Pygidium terminal, opening between a pair of thick, digitiform anal cirri, with dorsal anus (Fig. 4G). Pygidial cirrus extending to the last five chaetigers. Ventral cirrus of the last chaetiger with short cirrophores, ~10% of the total length of cirrostyle (Fig. 4G).

Parapodia well developed with widely separated rami in all chaetigers (Fig. 4A and D). Parapodia birramous, notopodia with short accessory and dorsal cirri and neuropodia with single ventral cirrus. First and second chaetigers with lobes reduced in size and directed dorsally, with fascicles of gross bidentate chaetae facing to the back (Fig. 4A). Neuropodial cirri of second chaetiger long, with short ceratophore, reaching chaetiger 6 (Fig. 4C).

Notochaetae change along the body, of four types: (i) smooth, bifurcate chaetae, erected dorsally (Fig. 6A, Fig. 7A–D), present on first four chaetigers; (ii) thick, bowed, bifurcate chaetae (20–25 in number, all smooth and shorter than that of the length to dorsal and accessory

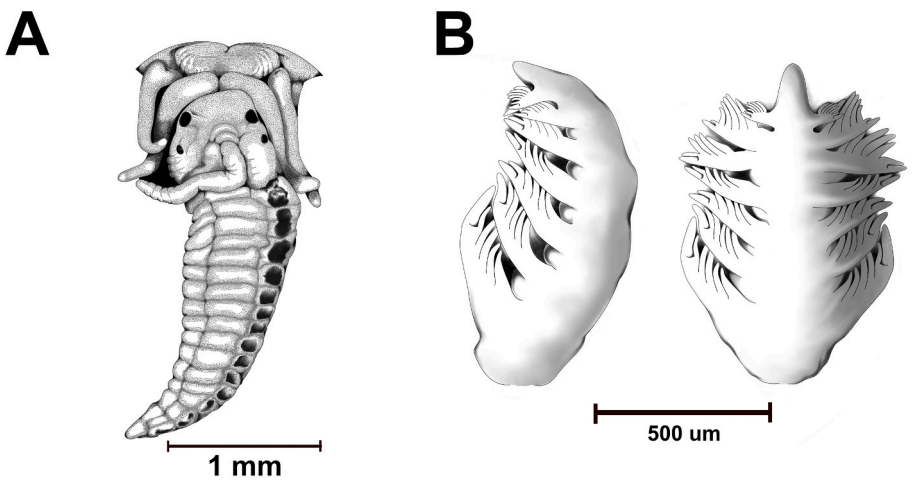

Fig. 5. *Chloeia rozbaczyloi* sp. nov. **A,** Drawing of the anterior end, dorsal view of the prostomium and the caruncle, which is presented in a laterodorsal position to show the number of vertical folds; **B** Lateral and frontal view of bipinnate branchiae of mid chaetigers.

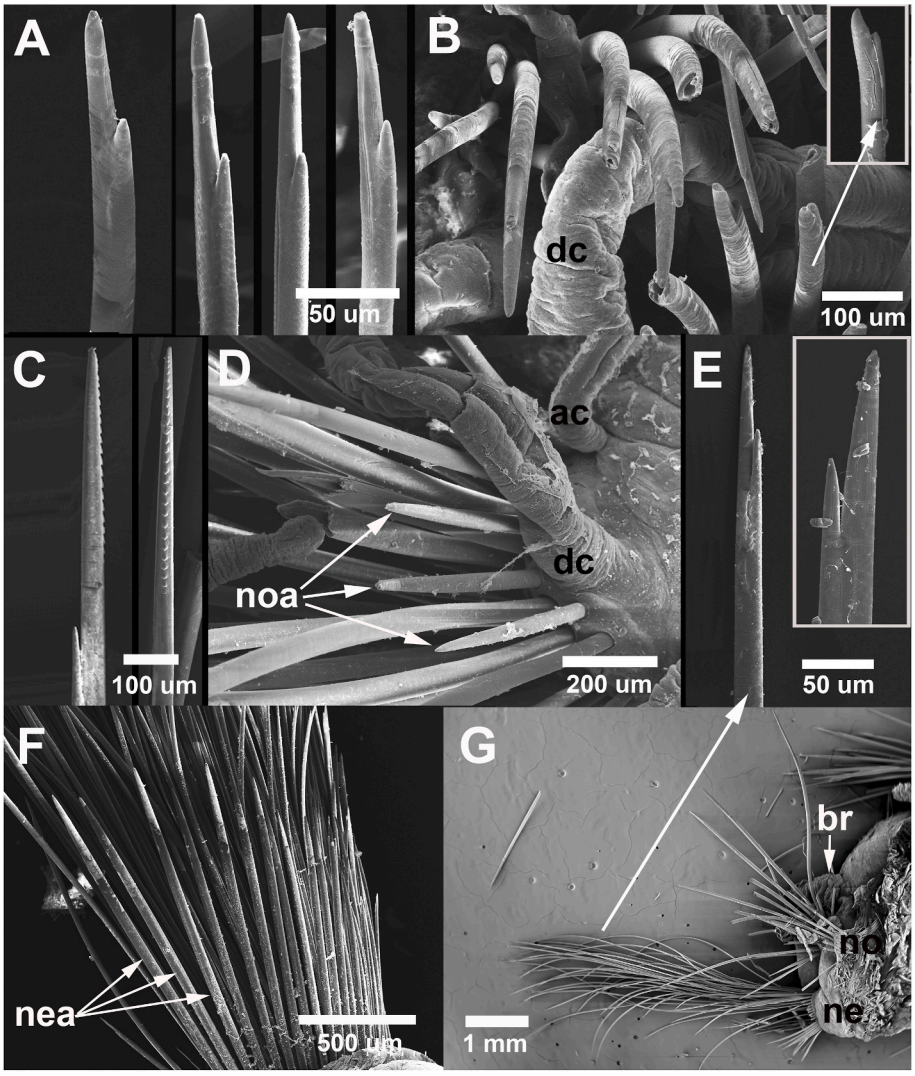

Fig. 6. SEM images of *Chloeia rozbaczyloi* sp. nov. notochaetae. **A** Smooth, bifurcate chaetae, erected dorsally; **B** bowed, bifurcated notochaetae of anterior parapodia, showing an insert of the distal end of this chaetae (dc = dorsal cirrus); **C** bifurcate harpoon notochaetae with serrated edge of medium and posterior parapodium; **D** notoaciculae of third chaetiger (noa = notoaciculae, ac = accessory cirri). Neurochaetae: **E** distal end of thin, bifurcated neurochaetae of mid chaetigers in two positions to show the proportion between main fang and secondary tooth: **F** bundle of posterior neurochaetae and disposal of neuroaciculae (nea); **G** anterior view of posterior parapodium showing differences in abundance and length between dorsal and ventral neurochaetae (br = branchiae, no = notopodium, ne = neuropodium).

cirri) with distal end stout and directed toward the posterior end of the body (Fig. 6B; Fig. 7E–F), present up to chaetiger 4; (iii) bifurcate harpoon with serrated outer edge present from fifth chaetiger onward; 30 to 35 per notopodium in mid chaetigers; secondary fang is one-third the length of the main fang; deep groove between both fangs; serrated zone with 24–27 lateral serrations (Fig. 6C; Fig. 7G–H); and (iv) short,

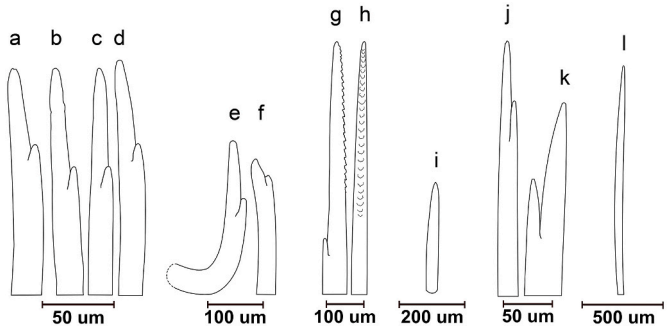

Fig. 7. *Chloeia rozbaczyloi* sp. nov chaetae types: **a-d** smooth, anterior bifurcate chaetae; **e-f** bowed, bifurcated notochaetae of anterior parapodia; **g-h** bifurcate harpoon notochaetae with serrated edge in two position; **i** notoaciculae of anterior chaetiger; **j-k** distal end of thin, bifurcated neurochaetae of mid chaetigers in two positions to show the proportion between main fang and secondary tooth: **l** neuroaciculae of mid chaetiger.

stout, unidentate chaetae with acicular shape, three to five in number and located dorsally to notochaetae fascicle (Fig. 6D; Fig 7I).

Neurochaetae white in color, finer, longer and more abundant relative to notochaetae (~11:3 in abundance). Dorsal neurochaetae longer than ventral neurochaetae. Neurochaetae of three types: (i) thin, long and distally bifurcated with short distance and deep groove between main fang and secondary tooth (Fig. 6E; Fig. 7J–K), around 70 to 90 chaetae per dorsal neuropodium; (ii) less abundant, short, stout, bidentate located ventrally and positioned posterior to ventral cirrus, around 20 per neuropodium, acicular chaetae not present in this bundle (Fig. 6F); and (iii) unidentate chaetae with acicular shape that encircle the long, bifurcate chaetae, between seven to fifteen by neuropodium (Fig. 6G; Fig 7L). Neuroaciculae abundance increments from anterior to posterior segments. Ceratophore of neuropodium inserted after and down of the ventral fascicle of neurochaetae (Fig. 6G). Length of neurochaetae and dorsal cirrus relatively similar. Neurochaetae in the last four chaetigers short, less abundant and not exceeding the distal end of the pygidial cirri (Fig. 6G).

Taxonomic remarks. Traditionally, *Chloeia* species have been separated by their dorsal pigmentation patterns, the number of the chaetiger where branchiae start, and the relative length of ventral cirri of chaetiger 2 (Horst, 1912). Recently, new features have been added, such as the size proportion between anterior and posterior eyes, the type of branchial ramification (pinnate vs. bipinnate), size trends of branchiae along the body, and the type of chaetae present (Yáñez-Rivera and Salazar-Vallejos, 2022; Salazar-Vallejo, 2023). The taxonomic arrangement of the 43 currently valid species of *Chloeia* (including *C. rozbaczyloi* sp. nov.) (Read and Fauchald, 2022; Yáñez-Rivera and Salazar-Vallejo, 2022; Salazar-Vallejo, 2023) is summarized in Table 1.

According to morphological characteristics, Salazar-Vallejo (2023) established five groups for *Chloeia* species (Table 1) and named each after their typical species (i.e. *flava, venusta, viridis, tumida,* and *kudenovi*). Species in the *venusta* group present bippinate branchiae from chaetiger 4, progressively decreasing in size, and a single middorsal band (Salazar-Vallejo, 2023). The *venusta* group currently includes *C. nuriae C. piotrowskiae*, *C. poupini,* and *C. venusta.* According to the above-mentioned characteristics, *C. rozbaczyloi* sp. nov. fits into this group.

Within the *venusta* group, *Chloeia rozbaczyloi* sp. nov. differs from *C. nuriae* (Gulf of California to Ecuador) because the latter species has anterior eyes that are 3 × larger than posterior ones, a reddish middorsal, a noncontinuous longitudinal band, and a black caruncle tapered with 21 vertical folds. *Chloeia piotrowskiae* (Philippines) differs in having a regular middorsal band not constricted posteriorly, a caruncle with plicate median ridge and about 30 vertical folds (most marked by dorsal, abundant blackish spots), partially concealing lateral lobes, and bipinnate branchiae in median segments with 14–16 lateral branches, each with few secondary filaments. *Chloeia rozbaczyloi* sp. nov. differs from *C. poupini* (French Polynesia) by the latter species having a blackish anterior prostomial area; a wide middorsal band that is continuous along each segment and that is medially separated along a few anterior chaetigers; a caruncle that is darker than the adjacent body wall, that is contracted, bent laterally, reaching chaetiger 4, that is without dorsal black spots but has a median ridge with about 30 vertical folds; and median segments with branchiae with 7–8 lateral branches, each with few secondary filaments. *Chloeia venusta* (Northeastern Atlantic to Morocco and Italy) differs in having a prostomium that is anteriorly entire, pairs of minute, blackish eyes (anterior pair is slightly larger than the posterior ones), and a caruncle that is pale, slightly surpassing chaetiger 4, with a line of 12 coalescent spots and a plicate median ridge with about 25 vertical folds.

In *Chloeia rozbaczyloi* the caruncle reaches chaetiger 4, with a median plicate lobe with 16–20 vertical folds and with 10–14 dorsal black spots, decreasing in size to the posterior end.

The following key is proposed to identify *Chloeia* species of the *venusta* group:

1a. Caruncle median ridge with ≤ 20 vertical folds	*C. rozbaczyloi* sp. *nov.*
1b. Caruncle median ridge with ≥ 20 vertical folds	2
2a (1b) Caruncle with 21–25 vertical folds	3
2b (1b) Caruncles with > 25 vertical folds	4
3a (2a) Anterior eyes about 8 × larger than posteriors	*C. nuriae*
3b (2a) Eyes minute, anterior eyes slightly larger than posterior ones	*C. venusta*
4a (2b). Branchiae with 14–16 lateral branches	*C. piotrowskiae*
4b (2b). Branchiae with 7–8 lateral branches	*C. poupini*

The known bathymetric range of *Chloeia rozbaczyloi* sp. nov. (211–230 m depth) is much restricted compared with other central and eastern Pacific species (e.g. *C. murrayae*, 30–200 m depth; *C. nuriae*, 13–210 m depth; *C. pseudeglochis*, 12–270 m depth), but is close to that of *C. pinnata* (166–305 m depth) and shallower than *C. poupini* (860 m depth) (Salazar-Vallejo, 2023).

Meristic remarks. The total number of analyzed individuals = 64. Average length: 26.5 ± 7.2 mm (mean ± SD); average wet weight: 0.4 ± 0.3 g; average number of segments: 30 ± 1.6 segments. Total weight (TW)-Length (TL) relationship was: $TW = 0.0945\ e^{0.0532\ TL}$; $r^2 = 0.5951$) and the total length (TL) versus the number of segments (NS) was: NS = 0.1345 TL + 26.415; $r^2 = 0.3772$. *Chloeia rozbaczyloi* nov. sp. could be considered a mid-sized species (up to 50 mm in total length). Although some shallow-waters species attain a rather large size (*C. tumida*, 162 mm in length; *C. flava*, 140 mm), the trend is that deep-water species tend to be smaller (>500 m depth; < 24 mm length) (Salazar-Vallejo, 2023). *Chloeia rozbaczyloi* sp. nov. differs in its larger size (26.5 ± 7.2 mm length) and higher number of chaetigers (26–35) than other deep-water species *C. kudenovi* (750–1045 m; 24 mm; 24 chaetigers), *C. pocicola* (~750 m; 6–20 mm length, 17 to 24 chaetigers), and *C. fiegei* (740–745 m; 22 mm, 28 chaetigers). Additional morphometric parameters based on SEM photos of a paratype specimen (SCBUCN 6982) for *C. rozbaczyloi* sp. nov. are presented in Supplementary Material Table S8.

Etymology. The species is named after Prof. Nicolás Rozbaczylo, for his outstanding dedication and notable contributions to the taxonomy and ecology of Chilean Polychaeta since 1973.

Geographic and bathymetric distribution. Only known from the type locality (seamount SFX, 25.079°S, 82.006°W, ~220 m depth) and from seamount SPG4 (25.408°S, 81.769°W, ~211 m depth), both within the NDMP.

3.2. Genetic analyses

A 7294 bp fragment containing the complete *18S* rRNA gene, ITS1,

the complete 5.7S rRNA gene, ITS2, and a partial 28S rRNA gene (GenBank accession OM 135245) and a 16,395 bp (estimated length) partial mitochondrial genome (OM 144973) of *C. rozbaczyloi* sp. nov. were recovered. Unrecovered regions of the mitochondrial genome include (1) an estimated 34 bp of the *COX2* gene, (2) an unknown number of bases in the intergenic region containing the control region (between the *COX3*-tRNA^{Lys} and tRNA^{Gln}-*ND6* genes), (3) an estimated 24 bp in the *ND5* gene, and (4) an estimated 450 bp from the *ND4L* gene (estimated 171 bp missing) into the *ND4* gene (estimated 286 bp missing) (Supplementary Material Table S7). Numerous ambiguities were present in the intergenic region containing the control region that likely represents differences between copies of a 730 bp repeated region (Supplementary Material Table S7). The recovered mitochondrial genome consists of 13 protein-coding genes, 23 tRNA genes, and 2 rRNA genes and had a nucleotide composition of 29.5% A, 22.0% C, 13.7% G, and 34.8% T (excluding missing and ambiguous bases). GC content of the complete mitochondrial genome (less missing bases) was 35.7%, and GC content of genes were 20.0–46.2% (Supplemental Material Table S7). Protein-coding genes terminated in a TAA codon or an incomplete codon (T–), and, except for the *ND2* gene, amino acid sequence similarity was higher than nucleotide similarity when compared to *C. pocicola* (Supplemental Material Table S7).

Bayesian and ML phylogenetic reconstruction based on the concatenated *28S* rRNA, *16S* rRNA, and *COI* gene fragments recovered a *Chloeia* clade sister to the *Notopygos* clade with moderate (>90 PP, > 70 BP) to strong (>95 PP, > 85 BP) support for the relationships among *Chloeia* species, except for *Chloeia pocicola*, the most basal species in the *Chloeia* clade (Fig. 8). *Chloiea rozbaczyloi* sp. nov. was basal to the other *Chloeia* species and was most genetically similar to *C. bimaculata* (95.4%) and *C. viridis* (95.2%) based on the concatenated alignment; within *Chloiea*, interspecific genetic distances were 2.4–8.5% (Supplementary Material Table S2). Alignments and reconstructed phylogenies based on each of the gene fragments likewise support *Chloiea rozbaczyloi* sp. nov. being in a clade with the other *Chloeia* spp. with genetic distances larger than reported for *Chloeia* spp. conspecifics and consistent with Chloeia interspecific values (Supplementary Material Tables S3–6 and Fig. S1). The evolutionary relationships among Archinominae genera *Chloeia*, *Archinome*, and *Notopygos* were not well supported (<85 PP, < 50 BP). In single-gene phylogenetic reconstructions (Supplementary Material Fig. S1), the evolutionary relationships within and among Archinominae genus clades differed.

4. Discussion

The description of *C. rozbaczyloi* sp. nov. currently increases the total number of species in the genus to 43 (Read and Fauchald, 2022; Salazar-Vallejo, 2023), and of the Chilean Amphinomidae species to seven, being the first formal species of the genus reported for the Nazca Ridge (Rozbaczylo, 1985; Cañete, 2017). *Chloeia rozbaczyloi* sp. nov. inhabits the Temperate South America biogeographic province (nr. 46 in Spalding et al., [2007]) and is the first report of the family for the Juan Fernández and Desventuradas Islands ecoregion (nr. 179). Future studies in this poorly explored area will reveal if the new species distributes in other seamounts than the two in which it has been recorded so far. However, Yáñez-Rivera and Salazar-Vallejo (2022) suggest that *Chloeia* from tropical and subtropical Eastern Pacific seem to have restricted geographic distributions, with notable diversification in the Indian and Indo-West Pacific Ocean.

Chloeia rozbaczyloi sp nov. seems to inhabit low-oxygen seamount ecosystems of the NDMP. At ~25°S the SE Pacific Oxygen Minimum Zone (OMZ) could intrude offshore to ~2000 km westward with a vertical extension >200m depth (Palma and Silva, 2006; Cañete and Häussermann 2012; Dewitte et al., 2021), reaching the summits of seamounts of the easternmost area of the NDMP. We speculate that lower bottom oxygen conditions were present at SFX (as indicated by the presence of numerous dead myctophids [Fig. 2G]) and could occur periodically in association with the seasonal fluctuation of the SE Pacific OMZ and westward drift of low-oxygen mesoscale eddies, which could relate to the relatively high abundance of *Chloeia rozbaczyloi* sp. nov. observed. Similar oceanographic and geological conditions seem to prevail on the easternmost Nazca Ridge seamounts (Palma and Silva, 2006; Fuenzalida et al., 2009; Dewitte et al., 2021). From an ecological approach, amphinomids constitute a group well known to thrive in benthic habitats overlaid by oxygen-deficient waters, be tolerant to hypoxia and thrive in reducing settings (Barroso and Paiva, 2011; Borda et al., 2015). For example, *Paramphinome australis* living at low oxygen concentrations of 0.52 ml L^{-1}, is the predominant polychaete along the Chilean continental margin at 400 m depth off the coast of Concepción, Chile (~36°S), comprising 42% of all polychaetes in this region (Gallardo et al., 2004). Other Archinomidae, including *Chloeia* species, are reported from regions with persistent OMZs, for which they may be well adapted in morphology and ecological function. For example, Purschke et al. (2017) reported that in the amphinomid *Eurythoe complanata*, ventilation is facilitated by longitudinal ciliary bands. Thus, the ciliated accessory dorsal cirri present in some species of *Chloeia*, including *C. rozbaczyloi* sp. nov., could likewise serve to provide enhanced ventilation where oxygen-deficient conditions prevail. Wang et al. (2019) also referred to accessory dorsal cirri functioning as branchial cirri. Notable abundances of *C. pinnata* are reported in offshore areas off California (Jones and Thompson, 1987) where persistent OMZ occurs and relatively strong currents result in the winnowing of finer detrital sediments and the development of coarse sediments rich in biogenic

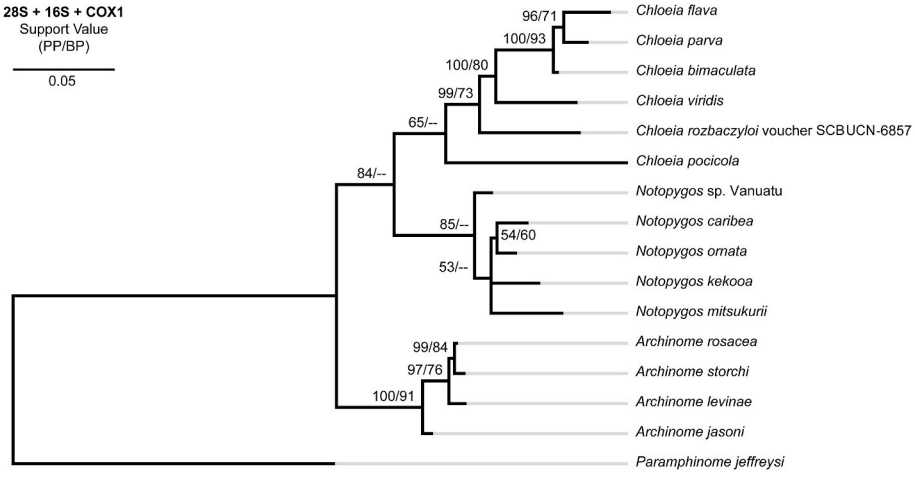

Fig. 8. Bayesian phylogenetic reconstruction (50% majority consensus) of Archinominae species with outgroup *Paramphinome jeffreysi* (Amphinominae) based on the 1492 bp alignment of *28S* rRNA + *16S* rRNA + *COI* codon position 1 and 2 gene fragments (735 + 323 + 394 bp, respectively) that provides support that *C. rozbaczyloi* sp. nov. is a distinct species from other *Chloeia* species for which these genetic markers are available. Support values are at the nodes with "–" indicating support of < 50 BP or a node not recovered in the maximum-likelihood analysis. Accession numbers and details of the specimens selected are available in Table S1. Commands for phylogenetic reconstructions are available in the "Scripts, job settings, and commands" section of the Supplementary Material.

calcium carbonate components.

In contrast to the low abundance and frequency of other amphinomids, such as *Linopherus annulata* that live in oxygenated waters in shallow estuarine areas of the Aysen fjord, southern Chile (Cañete et al., 1999), a comparatively high density of *C. rozbaczyloi* sp. nov. was observed on the summit of seamount SFX (Fig. 2B–F). In these habitats, polychaete species could play important ecological roles (e.g., carrion-feeding) as has been suggested for some amphinomid populations (mainly species of *Chloeia*) associated with sand and mud (Fauchald and Jumars, 1979; Salazar-Vallejo, 2023). This role may be substantially larger where amphinomids are locally abundant, such as in low-oxygen environments in which *C. pinnata* inhabits, and seamount SFX where *C. rozbaczyloi* sp. nov. is present. Potential food sources for *C. rozbaczyloi* sp. nov. include foraminifera and anthozoans, which were observed in large numbers at seamount SFX (Fig. 2A; Tapia-Guerra et al., 2021). Foraminifera have been reported as prey for *C. kudenovi* (Barroso and Paiva 2011) and *C. pinnata* (Jones and Thompson, 1987). Foraminifera contributed 11% to gut contents and were present in the guts of 37% of *C. pinnata* collected off the California coast (Jones and Thompson, 1987). Other species have been reported to prey on anthozoans (Fauchald and Jumars, 1979).

The only previous comprehensive study of the fauna of the Nazca and Salas y Gomez Ridges, conducted on 22 seamounts, was by Parin et al. (1997). Of the 192 species of benthic invertebrates reported in that study, 10 were polychaete taxa, among which the genus *Chloeia* is mentioned, but without providing any further taxonomic or ecologic details. Given the scarce knowledge of the deep-water fauna associated with seamounts within this area, it is too early to discuss the endemism patterns of the species described here. Nevertheless, its occurrence at only two seamounts of the seven seamounts sampled (ranging from 105 to 305 m depth) in the present study preliminarily suggests it has a limited distribution. Juan Fernández and the Desventuradas Islands bear among the highest endemicity levels in the world for coastal and shallow marine ecosystems (Friedlander et al., 2016; Wagner et al., 2021). Recent reports of potential endemism in this region include other benthic invertebrates, such as echinoderms (Mecho et al., 2020), new species of gastropods (Sellanes et al., 2019), and polychaetes (Díaz-Díaz OF et al., 2020), supporting the potential endemism for *Chloeia rozbaczyloi* sp. nov.

Chloeia rozbaczyloi sp. nov. is erected based on recent diagnostic taxonomic features and DNA analysis. From the morphological viewpoint, *Chloeia rozbaczyloi* sp. nov. can be distinguished from other species of the genus inhabiting the Pacific Ocean mainly by (i) the chromatic patterns of the dorsum (middorsal dark band, or *venusta* group, after Salazar-Vallejo (2023)) and the caruncle (with 16–20 vertical folds and between 12 and 14 black spots decreasing in diameter); (ii) by the bi-annulated dorsum of the first ten chaetigers, each with a bean-shaped anterior pseudosegment; (iii) long neuropodial cirri, with a short ceratophore, at chaetiger 2 and reaching chaetiger 6; and (iv) bipinnate branchiae from chaetiger 4, progressively decreasing in size to posterior end, with seven to nine lateral branches arising from the primary, with each possessing up to five pinnules. Prior studies have evaluated the phylogenetic relationship within Archinominae and Amphinomidae (Borda et al., 2012, 2015; Barroso et al., 2021) based on analyses of single-gene and concatenated gene datasets. Although the primary purpose of our phylogenetic analyses was to provide additional evidence to confirm the designation of *C. rozbaczyloi* sp. nov., the analyses were consistent with prior phylogenies in the lack of congruence between single-gene trees (Wang et al., 2019) and concatenated gene trees and the poor support for relationships among Amphinomidae genera. This lack of support may largely be due to the few representatives of each genus and family for which genetic data are available and outgroup selection (Lecointre et al., 1993; Graybeal, 1998). Therefore, without greater taxonomic coverage in phylogenetic reconstructions, the relationships among species and genera in phylogenetic trees may not reflect the true evolutionary history. Nevertheless, the data is sufficient to support *C. rozbaczyloi* sp. nov. being a distinct species from those with available genetic data. For example, the pairwise genetic distances between *C. rozbaczyloi* sp. nov. and its congeners (4.6–7.3) are comparable to or greater than those observed among the other *Chloeia* congeners (2.4–8.5) based on the concatenated data set (Supplementary Material Table S2). Single-gene alignments and phylogenetic reconstructions (Fig. S1) further support *C. rozbaczyloi* sp. nov. being a distinct species from those included in genetic analyses because the genetic distances are within the range of *Chloeia* interspecific genetic distances (2–20) and considerably larger than conspecific distances (<2) in *Chloeia* (Tables S3–6). Thus, *C. rozbaczyloi* sp. nov. is genetically distinct from congeners for which sequence data are available and it is most genetically similar to *C. bimaculata* and *C. viridis* (Fig. 6). Only one *Chloeia* species, *C. pocicola*, has a complete mitochondrial genome available for comparison to the mitochondrial genome of *C. rozbaczyloi* sp. nov. They have the same gene order, which differs from the other amphinomid mitochondrial genomes (*Eurythoe complanata* and *Cryptonome barbada*) in the position of the tRNA-Lys gene (Barroso et al., 2021). The presence of a large, repeated region with some differences in copies is also reported in *C. pocicola* (377 bp); however, it is nearly double the length in *C. rozbaczyloi* sp. nov. (730 bp). These data support that mitochondrial gene order is conserved within Amphinomidae as suggested by Barroso et al. (2021). Because we were unable to recover the complete mitochondrial genome, we cannot make further comparisons to amphinomid mitochondrial genomes. The dataset on *Chloeia* sequences is limited, covering only six of the 43 described species (Salazar-Vallejo 2023), so there remains a large potential to reconstruct the evolutionary history of this taxon and to understand how local ecological and evolutionary forces operate to govern the observed diversification in phenotype and genotype across different realms, provinces, and ecoregions (*sensu* Spalding et al., 2007), of the tropical, subtropical, and deep-sea habitats of the three oceans they occupy. Such potential is currently limited by the lack of inclusion of integrative systematics for species descriptions, such that species are still being described without the inclusion of some genetic data for support and comparison. Thus, systematics of Amphinomidae and all future descriptions should include at least some genetic data to fill this knowledge gap.

Seamount ecosystems are areas of high ecological relevance as they can harbor endemic and rare species, and provide suitable habitats to support the populations of many species of invertebrates and fishes (Friedlander et al., 2016). The present work increases the current knowledge of the biodiversity associated with the seamounts of the NDMP; however, further work is necessary to understand the role of this species in the ecosystem, its relationship with the OMZ, and to elucidate biogeographic connections within and among seamount ecosystems in this ecoregion as well as in others of the Southeastern Pacific Ocean.

Funding

This study was funded by: Comité Oceanográfico Nacional de Chile (CONA) grant C2216-09 to JS. ANID- Millennium Science Initiative ESMOI and ANID-ATE 22004 BiodUCCT, FONDEQUIP EQM150109, EQM160085, and FONDECYT 1181153 to JS and AM. Elaboration of the manuscript was partially supported by CONA-UMAG, Grant UMAG060807 CIMAR 26 Oceanic Island to JIC, OCEANA Chile provided the ROV and pilot.

Ethical approval

All applicable international, national, and/or institutional guidelines for the care and use of animals were followed by the authors.

Sampling and field studies

All necessary permits for sampling and observational field studies

have been obtained by the authors from the competent authorities and are mentioned in the acknowledgments.

Declaration of competing interest

The authors declare the following financial interests/personal relationships which may be considered as potential competing interests: Javier Sellanes, Ivan Canete reports financial support was provided by Comité Oceanográfico Nacional. Javier Sellanes, Erin E. Easton, Ariadna Mecho reports financial support was provided by Millennium Science Initiative ANID. Javier Sellanes reports financial support was provided by FONDEQUIP. Javier Sellanes, Ariadna Mecho reports financial support was provided by FONDECYT. Javier Sellanes reports equipment, drugs, or supplies was provided by OCEANA Chile.

Data availability

Supplementary genetic data included

Acknowledgments

The authors wish to thank the crew of the *AGS 61 Cabo de Hornos* for the facilities granted during the CIMAR 22 "Oceanic Islands" cruise. Special thanks also go to OCEANA for the support provided in the field with the ROV operation, and to María Valladares and EPIC cruise participants for field assistance. Jan M. Tapia-Guerra and Jorge Avilés (SCBUCN) are also acknowledged for help with Fig. 2. Marco León helped with the design of Figs. 5 and 7. Permit for sampling during the CIMAR 22 cruise was granted by Sub-secretaría de Pesca y Acuicultura, Chile, Resolution N° 3314. The comments and suggestions of three anonymous reviewers greatly helped to improve the manuscript.

Appendix A. Supplementary data

Supplementary data to this article can be found online at https://doi.org/10.1016/j.dsr.2023.104110.

References

Barroso, R., Paiva, P.C., 2011. A new deep-sea species of *Chloeia* (Polychaeta: Amphinomidae) from southern Brazil. J Mar Biol Ass UK 91 (2), 419–423.

Barroso, R., Kudenov, J.D., Shimabukuro, M., Carrerette, O., Sumida, P.Y.G., Paiva, P.C., Seixas, V.C., 2021. Morphological, molecular and phylogenetic characterization of a new *Chloeia* (Annelida: Amphinomidae) from a pockmark field. Deep-Sea Res. Part I 171 (17), 103499. https://doi.org/10.1016/j.dsr.2021.103499.

Bernt, M., Donath, A., Jühling, F., Externbrink, F., Florentz, C., Fritzsch, G., Pütz, J., et al., 2013. MITOS: improved de novo metazoan mitochondrial genome annotation. Mol. Phylogenet. Evol. 69, 313–319.

Böggemann, M., 2009. Polychaetes (Annelida) of the abyssal SE atlantic. Org. Divers. Evol. 9 (4), 251–428.

Borda, E., Kudenov, J.D., Bienhold, C., Rouse, G.W., 2012. Towards a revised Amphinomidae (Annelida, amphinomida): description and affinities of a new genus and species from the nile deep-sea fan, Mediterranean Sea. Zool. Scripta 41 (3), 307–325.

Borda, E.B., Yáñez-Rivera, B., Ochoa, G.M., Kudenov, J.D., Sánchez-Ortiz, C., Schulze, A., Rouse, G.W., 2015. Revamping Amphinomidae (Annelida: amphinomida), with the inclusion of *Notopygos*. Zool. Scripta 44, 324–333.

Cañete, J.I., Häussermann, V., 2012. Colonial life under Humboldt Current system: deep sea coral from O'Higgins I seamount. Lat Am J Aquat Res 40, 467–472.

Cañete, J.I., 2017. New record of *Pherecardia striata* (Polychaeta: Amphinomidae) from easter island, Chile. Lat Am J Aquat Res 45, 199–202.

Cañete, J.I., Leighton, G.L., Aguilera, F.F., 1999. Polychaetes from Aysén Fjord, Chile: distribution, abundance and biogeographical comparison with the shallow soft-bottom polychaete fauna from Antarctica and the Magellan Province. Sci. Mar. 63 (1), 243–252.

Dewitte, B., Conejero, C., Ramos, M., Bravo, L., Garcon, V., Parada, C., Sellanes, J., Mecho, A., Muñoz, P., Gaymer, C.F., 2021. Understanding the impact of climate change on the oceanic circulation in the Chilean island ecoregions. Aquat. Conserv. Mar. Freshw. Ecosyst. 31 (2), 232–252. https://doi.org/10.1002/aqc.3506.

Díaz-Díaz, O.F., Rozbaczylo, N., Sellanes, J., Tapia-Guerra, J.M., 2020. A new species of *eunice* cuvier, 1817 (Polychaeta: eunicidae) from the slope of the Desventuradas islands and seamounts of the Nazca Ridge, southeastern Pacific Ocean. Zootaxa 4860 (2), 211–226. https://doi.org/10.11646/zootaxa.4860.2.4.

Easton, E.E., Hicks, D., 2020. Complete mitogenome *of Carijoa riisei* (octocorallia: alcyonacaea: stolonifera: clavulariidae). Mitochondrial DNA Part. B. 5, 1826–1827. https://doi.org/10.1080/23802359.2020.1750998.

Fauchald, K., Jumars, P.A., 1979. The diet of worms: a study of polychaete feeding guilds. Oceanogr. Mar. Biol. 17, 193–284.

Felsenstein, J., 1981. Evolutionary trees from DNA sequences: a maximum likelihood approach. J. Mol. Evol. 17 (6), 368–376. https://doi.org/10.1007/BF01734359.

Friedlander, A.M., Ballesteros, E., Caselle, J.E., Gaymer, C.F., Palma, A.T., Petit, I., Varas, E., Muñoz, W., Sala, E., 2016. Marine biodiversity in juan Fernández and Desventuradas islands, Chile: global endemism hotspots. PLoS One. https://doi:10.1371/journal. Pone.0145059.

Fuenzalida, R., Schneider, W., Garcés-Vargas, J., Bravo, L., Lange, C., 2009. Vertical and horizontal extension of the oxygen minimum zone in the eastern South Pacific Ocean. Deep-Sea Res Pt II 56, 992–1003.

Gallardo, V.A., Palma, M., Carrasco, F.D., Gutiérrez, D., Levin, L.A., Cañete, J.I., 2004. Macrobenthic zonation caused by the oxygen minimum zone on the shelf and slope off Central Chile. Deep-Sea Res Pt II 51, 2475–2490.

Graybeal, A., 1998. Is it better to add taxa or characters to a difficult phylogenetic problem? Syst. Biol. 47 (1), 9–17.

Horst, R., 1912. In: Brill, E.J. (Ed.), Polychaeta Errantia of the Siboga Expedition, 24a, pp. 1–43.

Huelsenbeck, J.P., Ronquist, F., 2001. MRBAYES: Bayesian inference of phylogenetic trees. Bioinformatics 17, 754–755. https://doi.org/10.1093/bioinformatics/17.8.754.

Jones, G.F., Thompson, B.E., 1987. The distribution and abundance of *Chloeia pinnata* Moore, 1911 (Polychaeta: Amphinomidae) on the southern California borderland. Pac. Sci. 41, 122–131.

Kohn, A., Lloyd, M.C., 1973. Marine polychaetes annelids of eastern island. Int. Rev. Hydrobiol. 58, 691–712.

Kudenov, J., 1991. A new family and genus of the order Amphinomida (Polychaeta) from Galapagos hydrothermal vents. Ophelia 5, 111–120.

Kudenov, J., 1993. Amphinomidae and euphrosinidae (Annelida: Polychaeta) principally from Antarctica, the southern ocean and subantarctic region. Antarct. Res. 58, 93–154.

Kudenov, J., 1995. Family Amphinomidae Lamarck, 1818. Tax. Atlas of the Benthic Fauna of the Santa Maria Basin and West. Santa Barbara Channel 5, 207–215.

Lamarck, J.B., 1818. Histoire naturelle des animaux sans vertèbres 5, 1–612.

Lanfear, R., Calcott, B., Ho, S.Y., Guindon, S., 2012. Partitionfinder: combined selection of partitioning schemes and substitution models for phylogenetic analyses. Mol. Biol. Evol. 29 (6), 1695–1701. https://doi.org/10.1093/molbev/mss020, 2012 Jun.

Lanfear, R., Frandsen, P.B., Wright, A.M., Senfeld, T., Calcott, B., 2017. PartitionFinder 2: new methods for selecting partitioned models of evolution for molecular and morphological phylogenetic analyses. Mol. Biol. Evol. 34 (3), 772–773. https://doi.org/10.1093/molbev/msw260, 2017 Mar 1.

Lecointre, G., Hervé, G., Hoc LanhVan, L., Le Guyader, H., 1993. Species sampling has a major impact on phylogenetic inference. Mol. Phylogenet. Evol. 2 (3), 205–224.

Liñero-Arana, I., Díaz, O., 2010. Amphinomidae and euphrosinidae (Annelida: Polychaeta) from northeastern coast of Venezuela. Lat Am J Aquat Res 38, 107–120.

McIntosh, W.C., 1885. Report of the Annelida Polychaeta collected by H. M. S. Challenger during the years 1873-76. Challenger Rep 12, 1–554.

Orrhage, L., 1990. On the microanatomy of the supraoesophageal ganglion of some amphinomids (Polychaeta Errantia), with further discussion of the innervation and homologues of the polychaete palps. Acta Zool-Stockholm 71, 45–59.

Palma, S., Silva, N., 2006. Epipelagic siphonophore assemblages associated with water masses along a transect between Chile and Easter Island (eastern South Pacific Ocean). J. Plankton Res. 28, 1143–1151.

Parin, N., Mironov, A.N., Nesis, K.N., 1997. Biology of the Nazca and sala y Gomez submarine ridges, an outpost of the Indo- West Pacific fauna in the eastern Pacific Ocean: composition and distribution of the fauna, its communities and history. Adv. Mar. Biol. 32, 145–242. https://doi.org/10.1016/S0065-2881(08)60017-6.

Purschke, G., Hugenschu tt, M., Ohlmeyer, L., Meyer, H., Weihrauch, D., 2017. Structural analysis of the branchiae and dorsal cirri in *Eurythoe complanata* (Annelida, Amphinomida). Zoomorphology 136, 1–18.

Read, G., Fauchald, K. (Eds.), 2022. World Polychaeta Database. *Chloeia* Lamarck, p. 1818. World Register of Marine Species at: https://www.marinespecies.org/aphia.php?p=taxdetailsandid=129184 on 2022-11-30.

Rouse, G.W., Pleijel, F., 2001. Polychaetes. University Press, Oxford.

Rozbaczylo, N., 1985. Los anélidos poliquetos de Chile. Índice sinonímico y distribución geográfica de especies. In: Monografías Biológicas, 3. Pontificia Universidad Católica de Chile, pp. 1–284.

Salazar-Vallejo, S.I., 2023. Revision of *Chloeia* Savigny in Lamarck, 1818 (Annelida, Amphinomidae). Zootaxa 5238, 1–134.

Sellanes, J., Salisbury, R.A., Tapia, J.M., Asorey, C.M., 2019. A new species of *atrimitra* dall, 1918 (gastropoda: mitridae) from seamounts of the recently created nazca-desventuradas marine Park, Chile. PeerJ 7, e8279. https://doi.org/10.7717/peerj.8279.

Spalding, M.D., Fox, H.E., Allen, G.R., Davidson, N., Ferdaña, Z.A., Finlayson, M., Halpern, B.S., Jorge, M.A., Lombana, A., Lourie, S.A., Martin, K.D., McManus, E., Molnar, J.R., Recchia, C.A., Robertson, J., 2007. Marine ecoregions of the world: a bioregionalization of coastal and shelf areas. Bioscience 57, 573–583.

Stamatakis, A., 2014. RAxML version 8: a tool for phylogenetic analysis and post-analysis of large phylogenies. Bioinformatics 30 (9), 1312–1313.

Tapia-Guerra, J.M., Mecho, A., Easton, E.E., Gallardo, M.A., Gorny, M., Sellanes, J., 2021. First description of deep benthic habitats and communities of oceanic islands and seamounts of the Nazca Desventuradas Marine Park, Chile. Sci. Rep. 11, 6209. https://doi.org/10.1038/s41598-021-85516-8.

Wang, Z., Zhang, Y., Xie, Y.J., Qiu, J.-W., 2019. Two species of fire worms (Annelida: Amphinomidae: *Chloeia*) from Hong Kong. Zool. Stud. 58 https://doi.org/10.6620/ZS.2019.58-22.

Wagner, D., van der Meer, L., Gorny, M., Sellanes, J., Gaymer, C., Soto, E.H., Easton, E.E., Friedlander, A.M., Lindsay, D.J., Molodtsova, T.N., Boteler, B., Durussel, C., Gjerde, K.M., Currie, D., Gianni, M., Brooks, C.M., Shiple, M.J., Wilhelm, T.A., Quesada, M., Thomas, T., Dunstan, P.K., Clark, N.A., Villanueva, L.A., Pyle, R.L., Clark, M.R., Georgian, S.E., Morgan, L.E., 2021. The Salas y Gómez and Nazca ridges: a review of the importance, opportunities and challenges for protecting a global diversity hotspot on the high seas. Mar. Pol. 126, 194377 https://doi.org/10.1016/j.marpol.2020.104377.

Xia, X., 2018. DAMBE7: new and improved tools for data analysis in molecular biology and evolution. Mol. Biol. Evol. 35 (6), 1550–1552. https://doi.org/10.1093/molbev/msy073.

Xia, X., Lemey, P., 2009. Assessing substitution saturation with DAMBE. In: Lemey, P., Salemi, M., Vandamme, A. (Eds.), The Phylogenetic Handbook: A Practical Approach to Phylogenetic Analysis and Hypothesis Testing. Cambridge University Press, Cambridge, pp. 615–630. https://doi.org/10.1017/CBO9780511819049.022.

Xia, X., Xie, Z., Salemi, M., Chen, L., Wang, Y., 2003. An index of substitution saturation and its application. Mol. Phylogenet. Evol. 26, 1–7, 2003.

Yáñez-Rivera, B., Salazar-Vallejo, S.I., 2022. Revision of *Chloeia* Savigny in Lamarck, 1818 from tropical American seas (Annelida, Amphinomidae). Zootaxa 5128, 503–537.